JACS
JOURNAL OF THE AMERICAN CHEMICAL SOCIETY
Communication
pubs.acs.org/JACS

Ligand Mediated Transformation of Cesium Lead Bromide Perovskite Nanocrystals to Lead Depleted Cs_4PbBr_6 Nanocrystals

Zeke Liu,[†,‡,∥] Yehonadav Bekenstein,[‡,∥] Xingchen Ye,[‡] Son C. Nguyen,[‡] Joseph Swabeck,[‡,∥] Dandan Zhang,[‡,∥] Shuit-Tong Lee,[†] Peidong Yang,[‡,§,∥,⊥] Wanli Ma,*[,†] and A. Paul Alivisatos*[,‡,§,∥,⊥]

[†]Institute of Functional Nano & Soft Materials (FUNSOM), Collaborative Innovation Center of Suzhou Nano Science and Technology, Soochow University, Suzhou, Jiangsu 215123, China

[‡]Department of Chemistry, University of California Berkeley, Berkeley, California 94720, United States

[§]Department of Materials Science and Engineering, University of California Berkeley, Berkeley, California 94720, United States

[∥]Materials Sciences Division, Lawrence Berkeley National Laboratory, Berkeley, California 94720, United States

[⊥]Kavli Energy NanoScience Institute, University of California Berkeley and Lawrence Berkeley National Laboratory, Berkeley, California 94720, United States

Supporting Information

ABSTRACT: Lead halide perovskite nanocrystals (NCs) have emerged as attractive nanomaterials owing to their excellent optical and optoelectronic properties. Their intrinsic instability and soft nature enable a post-synthetic controlled chemical transformation. We studied a ligand mediated transformation of presynthesized $CsPbBr_3$ NCs to a new type of lead−halide depleted perovskite derivative nanocrystal, namely Cs_4PbBr_6. The transformation is initiated by amine addition, and the use of alkyl-thiol ligands greatly improves the size uniformity and chemical stability of the derived NCs. The thermodynamically driven transformation is governed by a two-step dissolution−recrystallization mechanism, which is monitored optically. Our results not only shed light on a decomposition pathway of $CsPbBr_3$ NCs but also present a method to synthesize uniform colloidal Cs_4PbBr_6 NCs, which may actually be a common product of perovskite NCs degradation.

Postsynthetic chemical transformations, such as ion-exchange reactions,[1] galvanic replacement,[2] or the nanoscale Kirkendall effect,[3] can be easily realized in colloidal nanocrystals (NCs) due to their high surface-to-volume ratios and short diffusion path lengths. These transformations give access to a myriad of novel structures that are difficult or impossible to synthesize directly. Lead−halide perovskite NCs including organic−inorganic hybrid perovskites, $CH_3NH_3PbX_3$ (X = Cl, Br, I),[4] and all-inorganic perovskites, $CsPbX_3$,[5] have emerged as attractive optoelectronic semiconductors. Ion-exchange transformations have been successfully applied to create various halide compositions of perovskite NCs owing to the high migration mobility of the halide anions.[6]

The ionic nature of lead halide perovskites results in their chemical instability in polar solvents.[7] As a result, it is also more challenging to find the right conditions for exchanging their surface ligands compared to traditional II−VI, III−V, and IV−VI semiconducting NCs, commonly leading to crystal degradation. Understanding the degradation mechanism of these NCs is therefore a prerequisite for implementation in real-life applications. Meanwhile, the "soft nature" (high ion mobility[8] and dynamic surface ligand binding[9]) of lead perovskite NCs position them as interesting candidates for studying chemical and crystallographic transformations.

Two stable compounds exist in the phase diagram of a mixed system of $CsX-PbX_2$ (X = Cl, Br), the incongruent ternary compounds Cs_4PbX_6 and the congruent compounds $CsPbX_3$.[10] The different crystal structures of $CsPbX_3$ and the lower-symmetry, lead−halide depleted Cs_4PbX_6 are highlighted in Figure 1. In Cs_4PbX_6, the $PbBr_6^{4-}$ octahedra are separated by

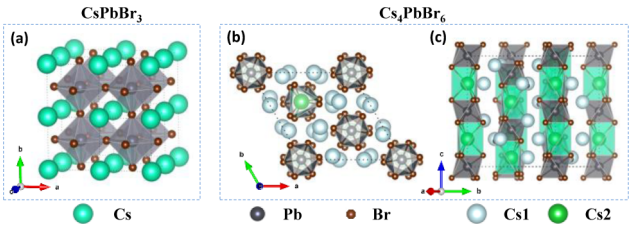

Figure 1. Schematic crystal structure of (a) $CsPbBr_3$ and Cs_4PbBr_6 (b) along and (c) perpendicular to *c* axis.

$Cs^+(2)$ trigonal prisms (there are two distinct kinds of Cs^+ ions in Cs_4PbX_6 crystal, marked as (1) and (2)), forming one-dimensional $[CsPbX_6]_n^{3-}$ chains. These chains are further isolated from each other by $Cs^+(1)$ distorted dodecahedra (Figure 1b,c).[11] In contrast, $CsPbX_3$ possesses a higher symmetry simple cubic structure with connected corner-sharing $PbBr_6^{4-}$ octahedra (Figure 1a). Although there have been several reports on bulk Cs_4PbX_6,[10b,12] Cs_4PbX_6 NCs are less investigated, with only several reports[13] published during the review of this paper.

In this work, we represent a new type of chemical transformation from presynthesized $CsPbBr_3$ NCs to a lead−halide depleted perovskite derivative Cs_4PbBr_6 NCs. This

Received: February 9, 2017
Published: March 30, 2017

DOI: 10.1021/jacs.7b01409
J. Am. Chem. Soc. XXXX, XXX, XXX−XXX

transformation is governed by a two-step dissolution−recrystallization mechanism and mediated by alterations in the ligand shell environment. We study the effect of oleylamine (OLA) and various alkyl thiols. We find that OLA is essential to trigger the process, presumably facilitating the decomposition of $CsPbBr_3$ NCs through "ligand-assisted exfoliation".[14] Upon recrystallization, the presence of alkyl-thiol ligands will greatly improve the size uniformity and chemical stability of the derived Cs_4PbBr_6 NCs. We report the degradation pathway of $CsPbX_3$ NCs and present a new method to access stable uniform Cs_4PbBr_6 NCs.

Synthesis of $CsPbBr_3$ NCs was performed according to published protocols.[5a] The transformation process was carried out under ambient conditions at room temperature (Supporting Information (SI)). We found that the photoluminescence (PL) of initially bright $CsPbBr_3$ NCs was quenched upon adding alkyl thiols together with a trace amount of OLA. The emission loss is correlated with a morphological transformation from $CsPbBr_3$ nanocubes to polygonal NCs (Figure 2a−c). These newly

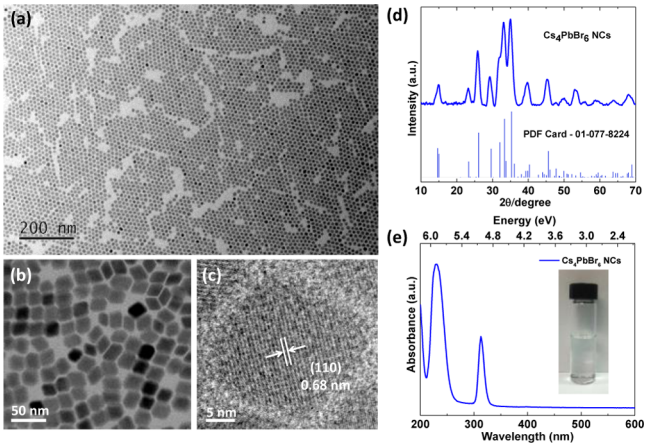

Figure 2. (a,b) Typical TEM image of Cs_4PbBr_6 NCs with different magnifications. (c) HRTEM of a single Cs_4PbBr_6 NC. (d) XRD spectra of trigonal phase Cs_4PbBr_6 NCs with $R\bar{3}c$ space group compared to the standard powder diffraction pattern of bulk Cs_4PbBr_6 ($\lambda_{Co\text{-}k\alpha}$ = 1.79 Å). (e) Absorption spectrum of Cs_4PbBr_6 NCs in hexane. Inset shows the photograph of the colorless Cs_4PbBr_6 NCs hexane solution.

derived NCs were characterized by X-ray diffraction (XRD), which matches the diffraction pattern of the rhombohedral Cs_4PbBr_6 phase (Figure 2d). Transmission electron microscopy (TEM) images show well-defined rhombus-shaped NCs (Figure 2b,c). The measured *d*-spacing of 0.68 nm from HRTEM (Figure 2c) agrees well with the {110} plane of rhombohedral Cs_4PbBr_6. The average size of the resulting Cs_4PbBr_6 NCs is ∼11.2 nm (Figure S1b).

The transformed Cs_4PbBr_6 NCs exhibit very different optical properties compared with the initial $CsPbBr_3$ NCs, showing two sharp absorbance peaks at 220 and 313 nm (Figures 2e and S2). These absorbance features match well with those of bulk thin film, which have been confirmed as the localized $6s_{1/2}$−$6p_{1/2}$ transitions within the individual $PbBr_6^{4-}$ octahedral separated by intervening Cs^+ ions.[11,15] The solution is transparent across the visible spectrum, presenting a distinctly colorless appearance (Figure 2e insert). Furthermore, room-temperature emission centered at 375 nm was observed upon 313 nm excitation, which is also in line with the optical measurements carried out on bulk Cs_4PbBr_6 thin films at low temperature (4.2 K).[10b] The luminescence quantum yield was reduced from as high as 70% for the initial $CsPbBr_3$ NCs to values near the detection limit of our apparatus for the final Cs_4PbBr_6 NCs. Although our results are consistent with many early reports,[10b,12a,15] we cannot ignore recent work on Cs_4PbBr_6 solids[16] and NCs,[13a] showing bright green emission at over 500 nm. Recently, Akkerman et al.[13b] have verified these green emissions were from residual doping and untransformed $CsPbBr_3$ NCs. We further tried this transformation in other halide perovskite NCs. For $CsPbCl_3$ NCs (Figure S3), this procedure produced pure Cs_4PbCl_6 NCs which show sharp absorbance peaks at 285 nm, which is also consistent with previous reports on the pure bulk and NCs.[12a,13b] However, we could not induce the transformation of $CsPbI_3$ NCs to Cs_4PbI_6 NCs.

The effect of different amines on the transformation was also investigated (Figure S4). Both 1-dodecanamine and 1-octylamine function similarly to OLA, giving Cs_4PbBr_6 NCs with nearly the same average size. However, 1-butylamine only gives a product with a very weak absorbance (that is also hard to observe in the TEM), and aniline results in a partial transformation. Additionally, Cs_4PbBr_6 NCs produced with shorter length thiols showed better stability than those with longer thiols. We further expanded the study of these transformations to also include alkyl dithiols with varying lengths. We observe all these can produce Cs_4PbBr_6 NCs. However, the NCs formed by using dithiols show better stability than those with monothiols (same carbon-chain length) (Figure S5). For example, Cs_4PbBr_6 NCs formed by using 1-dodecanethiol will partly transform back to initial $CsPbBr_3$ NCs, as indicated by the appearance of a PL peak at around 510−520 nm and XRD testing (Figure S6). In contrast, Cs_4PbBr_6 NCs produced by 1,3-propanedithiol (PDT) remain stable in hexane for several months without the reverse transformation occurring. In the following, we will focus on Cs_4PbBr_6 NCs created by PDT.

OLA was found to play a vital role in the transformation. As shown in Figure 3a, when we added OLA dropwise to the $CsPbBr_3$ NCs solution (PDT/Pb mol ratio =1300), the 492 nm absorption of $CsPbBr_3$ decreases with the concomitant increase of the 313 nm absorption arising from Cs_4PbBr_6 NCs. The

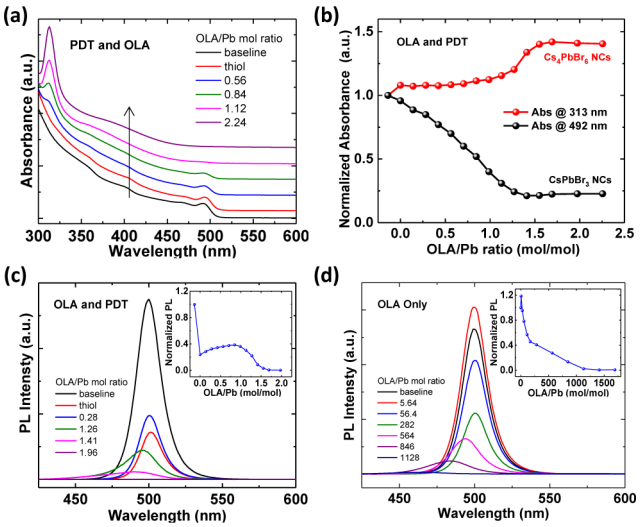

Figure 3. Effect of amount of OLA on the transformation behavior (a−c) with and (d) without PDT (see Figure S8 for absorbance). (a) Absorbance spectra. (b) Absorbance at two spectral features (492 and 313 nm). (c, d) PL spectra of $CsPbBr_3$ NCs solution after adding different amount of OLA.

DOI: 10.1021/jacs.7b01409
J. Am. Chem. Soc. XXXX, XXX, XXX−XXX

evolution of the absorbance at these two spectral positions are plotted in Figure 3b, showing inverse dependence on the OLA concentration. Before adding OLA, large amounts of PDT almost have no effect on the absorption spectrum (Figure 3a), showing that the thiol cannot trigger the transformation unaided. However, the addition of PDT will cause reduction of the PL intensity of $CsPbBr_3$ NCs by about 80% (Figure 3c). The progressive introduction of OLA initially restores the PL (OLA/Pb < 0.84). However, excess OLA (OLA/Pb > 0.84) leads to reduction in the PL intensity, accompanied by blue-shifting and an increase in the full width half-maximum of the emission peak, suggesting the decomposition of the $CsPbBr_3$ NCs. After the transformation and isolation of the Cs_4PbBr_6 NCs, yellow precipitates were observed. Energy dispersive X-ray spectroscopy (EDS) analysis of these products detected only Pb, Br, and S signals, which suggested that the complex is primarily composed of $PbBr_2$ and thiols (Figure S7). Therefore, the transformation process can be outlined in Scheme 1.

Scheme 1. Transformation Process

$$4CsPbBr_3 \xrightarrow{OLA+Thiol} Cs_4PbBr_6 + 3PbBr_2$$

We further investigated the thermodynamic boundaries of this transformation and found that pure excess OLA (more than 1000 times compared to the case with PDT) will also transform $CsPbBr_3$ to Cs_4PbBr_6 NCs (Figures 3d and S8). Markedly, the presence of PDT can largely reduce the amount of OLA required to trigger the transformation. This observation is rationalized by using hard–soft acid–base theory. Thiols bind strongly with $PbBr_2$ and precipitate it from solution, thermodynamically driving the reaction to the right side. Indeed, the immediate appearance of yellow precipitates when adding PDT to $PbBr_2$ solution supports this rationale. However, the size distribution and shape uniformity of the NCs produced by only OLA are of lower quality (Figure S9). Moreover, NCs formed without thiols are less stable and decompose as confirmed by XRD and the loss of the sharp absorbance around 313 nm (Figure S10). X-ray photoelectron spectroscopy (XPS), Fourier-transform infrared (FTIR), and nuclear magnetic resonance (NMR) were performed to study the surfaces of Cs_4PbBr_6 NCs (produced by both OLA and PDT). High-resolution XPS testing shows the signals of sulfur, which can be assigned to bound thiolate and unbounded thiol (or sulfite) (Figure S11b).[17] Meanwhile, FTIR spectra showed drastic differences between Cs_4PbBr_6 NCs and the initial $CsPbBr_3$ NCs (Figure S12). Specially, the peak around 800 cm^{-1} can be assigned to sulfur–metal bonds,[18] demonstrating that thiols serve as part of the capping ligands for the final Cs_4PbBr_6 NCs, which may be the reason for the improvement in their stability.

To further probe the mechanism of this transformation, we performed a kinetic study to monitor the reaction progression. The result from the *in situ* UV–vis absorption study is presented in Figure 4a. After injecting a solution mixture of PDT and OLA to a hexane solution of $CsPbBr_3$ NCs, the absorbance decreases immediately across the whole spectral range due to the concentration reduction. Afterward, the transformation process can be divided into two steps. First, the absorbance at 492 nm decreases to a constant value, which indicates the decomposition of $CsPbBr_3$ NCs (Figure S14a). This process persists for about 18 s, during which the PL intensity fluctuates (decreasing, increasing and decreasing again). The PL intensity was completely quenched after 15–20 s (Figure 4c,d), which

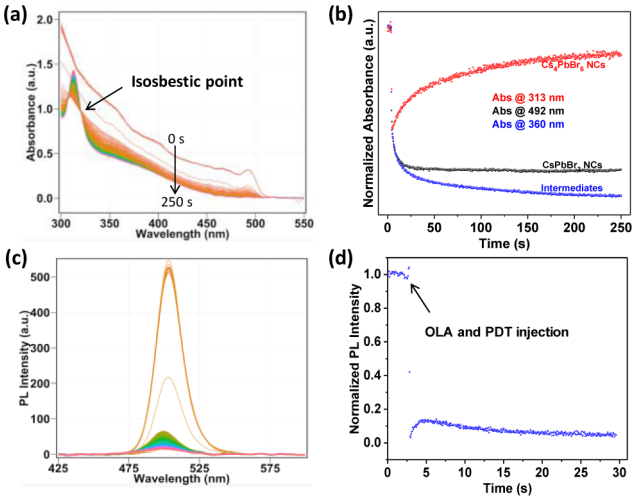

Figure 4. Optical monitoring of the transformation process from $CsPbBr_3$ NCs to Cs_4PbBr_6 NCs under treatment of OLA and PDT. (a) Time-resolved absorbance spectra. The time resolution is around 300 ms. (b) Temporal evolution of the absorbance at three spectral features in (a): 492, 360, and 313 nm. (c) Time-resolved PL spectra. The time resolution is around 80 ms. (d) Temporal evolution of PL intensity.

matches well with the time scale (18 s) for the absorbance to reduce to a constant value. The second step involves the development of a peak at 313 nm and a broad spectral feature in the region centered at around 360 nm (Figure S14b). The duration of this step is about 240 s. We plotted the evolution of the absorbance at three spectral positions (313, 360, and 492 nm) as a function of time during the whole transformation process (Figure 4b). The growing of the absorbance at 313 nm is concomitant with the decay of the 360 nm peak. A distinct isosbestic point appeared at 322 nm in the absorbance spectra (Figures 4a and S14b). The kinetic study of the transformation process with only OLA shows almost the same trend but with a much slower decomposition of $CsPbBr_3$ NCs (200 s compared to 18 s in the presence of PDT; see Figure S15). The existence of an isosbestic point indicates that one species is quantitatively transformed into another by complexation,[19] suggesting Cs_4PbBr_6 NCs are quantitatively transformed from some intermediates with an absorbance around 360 nm. Based on the investigation of complexation between $Pb^{2+}$and different amounts of Br^-,[20] the broad absorbance around 360 nm could be assigned to $[PbBr_4]^{2-}$, corresponding to a monolayer perovskite structure.[21] The existence of $[PbBr_4]^{2-}$ intermediates could be supported by the small amounts of sheet structures observed in the crude solution after transformation during TEM testing (Figure S16). The detailed mechanism of this process still requires further investigation and supporting data.

In conclusion, a ligand mediated controlled transformation of presynthesized $CsPbBr_3$ NCs to lead depleted perovskite derivative Cs_4PbBr_6 NCs was reported. While OLA by itself can trigger this process, we have found that by adding alkyl-thiol ligands the size uniformity and chemical stability of the Cs_4PbBr_6 NCs are greatly improved. This thermodynamic transformation process follows a two-step dissolution–recrystallization mechanism which we were able to resolve through optical spectroscopy. This postsynthetic chemical transformation is important in the greater context of improving the stability of lead–halide perovskites. Additionally, it serves as a practical method to achieve monodisperse Cs_4PbBr_6 NCs, broadening the library of metal–halide perovskite nanomaterials.

DOI: 10.1021/jacs.7b01409
J. Am. Chem. Soc. XXXX, XXX, XXX–XXX

■ ASSOCIATED CONTENT

Supporting Information

The Supporting Information is available free of charge on the ACS Publications website at DOI: 10.1021/jacs.7b01409.

Experimental details, particle characterization, detailed descriptions of fittings (PDF)

■ AUTHOR INFORMATION

Corresponding Authors

*wlma@suda.edu.cn

*alivis@berkeley.edu

ORCID

Yehonadav Bekenstein: 0000-0001-6230-5182

Son C. Nguyen: 0000-0001-7713-4195

Joseph Swabeck: 0000-0003-2235-2472

Shuit-Tong Lee: 0000-0003-1238-9802

Peidong Yang: 0000-0003-4799-1684

A. Paul Alivisatos: 0000-0001-6895-9048

Notes

The authors declare no competing financial interest.

■ ACKNOWLEDGMENTS

This work was supported by the U.S. Department of Energy, Office of Science, Office of Basic Energy Sciences, Materials Sciences and Engineering Division, under Contract No. DE-AC02-05-CH11231 within the Physical Chemistry of Inorganic Nanostructures Program (KC3103), by the National Key Research Projects (Grant No. 2016YFA0202402), the National Natural Science Fund (Grant No. 61674111), and the Priority Academic Program Development of Jiangsu Higher Education Institutions (PAPD). Z.L. thanks the National Postdoctoral Program for Innovative Talents (Grant No. BX201600113), State-Sponsored Scholarship for Graduate Students from China Scholarship Council. The authors kindly thank Dan Oron for his insightful ideas and also Brent A. Koscher, Matthew Koc, Alexander Buyanin, and Aizhao Pan for useful discussions, Rongbin Wang for XPS testing, and Hongyuan Jia for assisting the drawing process.

■ REFERENCES

(1) (a) Son, D. H.; Hughes, S. M.; Yin, Y.; Alivisatos, A. P. *Science* **2004**, *306*, 1009. (b) De Trizio, L.; Manna, L. *Chem. Rev.* **2016**, *116*, 10852.

(2) Xia, X.; Wang, Y.; Ruditskiy, A.; Xia, Y. *Adv. Mater.* **2013**, *25*, 6313.

(3) (a) Yin, Y.; Rioux, R. M.; Erdonmez, C. K.; Hughes, S.; Somorjai, G. A.; Alivisatos, A. P. *Science* **2004**, *304*, 711. (b) Wang, W.; Dahl, M.; Yin, Y. *Chem. Mater.* **2013**, *25*, 1179.

(4) (a) Schmidt, L. C.; Pertegas, A.; Gonzalez-Carrero, S.; Malinkiewicz, O.; Agouram, S.; Minguez Espallargas, G.; Bolink, H. J.; Galian, R. E.; Perez-Prieto, J. *J. Am. Chem. Soc.* **2014**, *136*, 850. (b) Vybornyi, O.; Yakunin, S.; Kovalenko, M. V. *Nanoscale* **2016**, *8*, 6278. (c) Protesescu, L.; Yakunin, S.; Bodnarchuk, M. I.; Bertolotti, F.; Masciocchi, N.; Guagliardi, A.; Kovalenko, M. V. *J. Am. Chem. Soc.* **2016**, *138*, 14202.

(5) (a) Bekenstein, Y.; Koscher, B. A.; Eaton, S. W.; Yang, P.; Alivisatos, A. P. *J. Am. Chem. Soc.* **2015**, *137*, 16008. (b) Protesescu, L.; Yakunin, S.; Bodnarchuk, M. I.; Krieg, F.; Caputo, R.; Hendon, C. H.; Yang, R. X.; Walsh, A.; Kovalenko, M. V. *Nano Lett.* **2015**, *15*, 3692. (c) Pan, A.; He, B.; Fan, X.; Liu, Z.; Urban, J. J.; Alivisatos, A. P.; He, L.; Liu, Y. *ACS Nano* **2016**, *10*, 7943. (d) Zhang, D.; Eaton, S. W.; Yu, Y.; Dou, L.; Yang, P. *J. Am. Chem. Soc.* **2015**, *137*, 9230.

(6) (a) Nedelcu, G.; Protesescu, L.; Yakunin, S.; Bodnarchuk, M. I.; Grotevent, M. J.; Kovalenko, M. V. *Nano Lett.* **2015**, *15*, 5635. (b) Akkerman, Q. A.; D'Innocenzo, V.; Accornero, S.; Scarpellini, A.; Petrozza, A.; Prato, M.; Manna, L. *J. Am. Chem. Soc.* **2015**, *137*, 10276. (c) Koscher, B. A.; Bronstein, N. D.; Olshansky, J. H.; Bekenstein, Y.; Alivisatos, A. P. *J. Am. Chem. Soc.* **2016**, *138*, 12065.

(7) Kim, Y.; Yassitepe, E.; Voznyy, O.; Comin, R.; Walters, G.; Gong, X.; Kanjanaboos, P.; Nogueira, A. F.; Sargent, E. H. *ACS Appl. Mater. Interfaces* **2015**, *7*, 25007.

(8) (a) Mizusaki, J.; Arai, K.; Fueki, K. *Solid State Ionics* **1983**, *11*, 203. (b) Eames, C.; Frost, J. M.; Barnes, P. R.; O'Regan, B. C.; Walsh, A.; Islam, M. S. *Nat. Commun.* **2015**, *6*, 7497.

(9) De Roo, J.; Ibanez, M.; Geiregat, P.; Nedelcu, G.; Walravens, W.; Maes, J.; Martins, J. C.; Van Driessche, I.; Kovalenko, M. V.; Hens, Z. *ACS Nano* **2016**, *10*, 2071.

(10) (a) Nitsch, K.; Cihlář, A.; Dušek, M.; Hamplová, V.; Nikl, M.; Rodová, M.; Ryšavá, N. *physica status solidi (a)* **1993**, *135*, 565. (b) Nikl, M.; Mihokova, E.; Nitsch, K.; Somma, F.; Giampaolo, C.; Pazzi, G.; Fabeni, P.; Zazubovich, S. *Chem. Phys. Lett.* **1999**, *306*, 280.

(11) Velázquez, M.; Ferrier, A.; Péchev, S.; Gravereau, P.; Chaminade, J.-P.; Portier, X.; Moncorgé, R. *J. Cryst. Growth* **2008**, *310*, 5458.

(12) (a) Kondo, S.-i.; Amaya, K.; Saito, T. *J. Phys. Soc. Jpn.* **2001**, *70*, 3751. (b) Kondo, S.; Masaki, A.; Saito, T.; Asada, H. *Solid State Commun.* **2002**, *124*, 211.

(13) (a) Zhang, Y.; Saidaminov, M. I.; Dursun, I.; Yang, H.; Murali, B.; Alarousu, E.; Yengel, E.; Alshankiti, B. A.; Bakr, O. M.; Mohammed, O. F. *J. Phys. Chem. Lett.* **2017**, *8*, 961. (b) Akkerman, Q. A.; Park, S.; Radicchi, E.; Nunzi, F.; Mosconi, E.; De Angelis, F.; Brescia, R.; Rastogi, P.; Prato, M.; Manna, L. *Nano Lett.* **2017**, *17*, 1924. (c) Udayabhaskararao, T.; Kazes, M.; Houben, L.; Teitelboim, A.; Oron, D. arXiv:1702.05382 [cond-mat.mtrl-sci].

(14) Hintermayr, V. A.; Richter, A. F.; Ehrat, F.; Doblinger, M.; Vanderlinden, W.; Sichert, J. A.; Tong, Y.; Polavarapu, L.; Feldmann, J.; Urban, A. S. *Adv. Mater.* **2016**, *28*, 9478.

(15) (a) Leguy, A. M. A.; Hu, Y.; Campoy-Quiles, M.; Alonso, M. I.; Weber, O. J.; Azarhoosh, P.; van Schilfgaarde, M.; Weller, M. T.; Bein, T.; Nelson, J.; Docampo, P.; Barnes, P. R. F. *Chem. Mater.* **2015**, *27*, 3397. (b) Christians, J. A.; Miranda Herrera, P. A.; Kamat, P. V. *J. Am. Chem. Soc.* **2015**, *137*, 1530.

(16) (a) Saidaminov, M. I.; Almutlaq, J.; Sarmah, S.; Dursun, I.; Zhumekenov, A. A.; Begum, R.; Pan, J.; Cho, N.; Mohammed, O. F.; Bakr, O. M. *ACS Energy Letters* **2016**, *1*, 840. (b) Rakita, Y.; Kedem, N.; Gupta, S.; Sadhanala, A.; Kalchenko, V.; Böhm, M. L.; Kulbak, M.; Friend, R. H.; Cahen, D.; Hodes, G. *Cryst. Growth Des.* **2016**, *16*, 5717. (c) Chen, D.; Wan, Z.; Chen, X.; Yuan, Y.; Zhong, J. *J. Mater. Chem. C* **2016**, *4*, 10646.

(17) (a) Tang, J.; Brzozowski, L.; Barkhouse, D. A. R.; Wang, X.; Debnath, R.; Wolowiec, R.; Palmiano, E.; Levina, L.; Pattantyus-Abraham, A. G.; Jamakosmanovic, D. *ACS Nano* **2010**, *4*, 869. (b) Cao, Y.; Stavrinadis, A.; Lasanta, T.; So, D.; Konstantatos, G. *Nature Energy* **2016**, *1*, 16035.

(18) (a) Reznickova, A.; Kolska, Z.; Siegel, J.; Svorcik, V. *J. Mater. Sci.* **2012**, *47*, 6297. (b) Li, Y.-S.; Li, S. *Spectrochim. Acta, Pt. A: Mol. Spectrosc.* **1994**, *50*, 509.

(19) (a) Schmidt, E.; Zhang, H.; Chang, C. K.; Babcock, G. T.; Oertling, W. A. *J. Am. Chem. Soc.* **1996**, *118*, 2954. (b) Yamamoto, K.; Higuchi, M.; Shiki, S.; Tsuruta, M.; Chiba, H. *Nature* **2002**, *415*, 509.

(20) (a) Oldenburg, K.; Vogler, A. *Zeitschrift für Naturforschung B* **1993**, 48. (b) Yoon, S. J.; Stamplecoskie, K. G.; Kamat, P. V. *J. Phys. Chem. Lett.* **2016**, *7*, 1368.

(21) (a) Mitzi, D. B. *Prog. Inorg. Chem.* **2007**, *48*, 1. (b) Weidman, M. C.; Seitz, M.; Stranks, S. D.; Tisdale, W. A. *ACS Nano* **2016**, *10*, 7830. (c) Gonzalez-Carrero, S.; Espallargas, G. M.; Galian, R. E.; Perez-Prieto, J. *J. Mater. Chem. A* **2015**, *3*, 14039.

DOI: 10.1021/jacs.7b01409
J. Am. Chem. Soc. XXXX, XXX, XXX−XXX